An Efficient Universal AC/DC Branch Model for Optimal Power Flow Studies in Hybrid AC/DC Systems

Mahmoud Shahbazi, *Senior Member, IEEE*

***Abstract*—This paper introduces a new efficient universal AC/DC branch model, *SADRA*, for modelling hybrid AC/DC systems in optimal power flow studies, with provisions of voltage and power controls. *SADRA* offers a versatile approach for modelling diverse AC, DC, and AC/DC elements including VSCs and VSC-interfaced elements (including point-to-point and multi terminal HVDC), phase-shifter and tap-changing transformers, and in general, hybrid AC/DC systems, all within a universal model. *SADRA* directly links AC and DC grids, and therefore it is able to use conventional AC equations for modelling. Moreover, it is capable of implementing VSC control actions as well. Due to its compact and simple structure, *SADRA* is fast and robust.**

To demonstrate *SADRA*'s performance, versatility, and speed, two large AC/DC systems with 1359 bus and 3125 buses are studied and the results are compared with the existing methods in the literature. It is shown that *SADRA* is a truly universal model, and also successfully implements voltage and power control actions. Additionally, it is demonstrated that in addition to its advantages, *SADRA* is as fast or faster than the comparable methods in recent literature, and is up to more than six times faster compared to models with control actions provisions.

***Index Terms*—Optimal power flow, AC/DC power systems, Power system modeling, Voltage source converter, HVDC transmission, Multi-terminal DC grids.**

NOMENCLATURE

α, β, γ	VSC power loss coefficients
τ	Tap ratio magnitude
θ	Tap ratio phase shift
θ_s	Phase angle of the slack bus (bus s)
C_f	Sparse connection matrix for *from* sides
C_t	Sparse connection matrix for *to* sides
i_f	Current at the *from* side
i_t	Current at the *to* side
k_d	Droop coefficient
N	Complex tap ratio
n_b	Number of buses
n_l	Number of branches
P_f	Active power at the *from* side
P_t	Active power at the *to* side
$P_{g_{dc}}$	Dummy generator active power
P_{loss}	VSC power loss
Q_f	Reactive power at the *from* side
Q_t	Reactive power at the *to* side
Q_{ac}	Reactive power at the AC side of VSC model
Q_{dc}	Reactive power at the DC side of VSC model
$Q_{g_{dc}}$	Dummy generator reactive power
S^i	Complex power injection at bus i
S^i_d	Complex demand at bus i
S^i_g	Complex power generated at bus i
S^i_l	Thermal power limit of line i
S_f	Vector of *from* side complex powers
S_t	Vector of *to* side complex powers
v_f	Voltage at the *from* side
v_t	Voltage at the *to* side
Y_f	Branch admittance matrix for *from* sides
Y_t	Branch admittance matrix for *to* sides
Y_{br}	2×2 branch admittance matrix

Mahmoud Shahbazi is with the Department of Engineering, Durham University, Durham, DH1 3LE, UK (email: mahmoud.shahbazi@durham.ac.uk).

I. INTRODUCTION

VOLTAGE Source Converter-based HVDC (VSC-HVDC) provides improved operational security, flexibility, reliability, and possibility of independent regulation of active and reactive powers [1], and therefore its use in shaping the modern power systems has accelerated recently [2] [3]. Renewable energy systems such as offshore wind farms also use VSC-HVDC as a solution for transporting power to the main grid. Many VSC-HVDC and several multi-terminal HVDC (MT-HVDC) systems are installed and many are planned [4] [5] [6] [7] [8]. These developments are accelerating the transition of modern power systems from AC to large-scale hybrid AC/DC [9].

Although the hybrid AC/DC power system is more flexible, it is also more complex. One of the most important means for determining optimal operating points in power systems is Optimal Power Flow (OPF). OPF is extremely important in operational and grid planning as well as in techno-economic studies. In OPF, the output power of the generators, their voltages, and other control settings such as transformer tap settings and VSC settings are determined by optimizing an objective function such as the total generation cost [10], while satisfying the system constraints.

OPF is a non-convex optimization problem due to the nonlinear power flow equations, as well as the operating constraints imposed by the AC/DC converters in hybrid AC/DC systems [10]. It is a very complex problem in general, and even more so in hybrid AC/DC systems.

Several OPF formulations for AC/DC hybrid systems are presented in the literature in recent years [11], [12]. Some of the earlier OPF algorithms such as [13], [14], [15] neglected

converter losses, or converter transformers and filters, or used linearized formulations of the AC and DC grids equations. In [1] DC and AC grids are modelled separately and then linked together. The converter losses are assumed to be proportional to the passing active power through the converter, while in most recent models more accurate quadratic converter losses are considered. In [16] OPF for hybrid AC/DC microgrids is studied and a new model for the interlinking converter is developed. Again, AC and DC subgrids are solved separately and then sequential methods are used to achieve feasible solutions for the original formulation. Moreover, in many of these studies, the OPF is implemented only for relatively small systems (for example up to 57 buses in [1] [17], up to 118 buses in [16], [18] and [10]) and therefore its scalability is not known.

An OPF framework is presented in [9] and a state space relaxation is introduced that relaxes the state of DC subgrids to voltage phasors, for a unified OPF formulation using AC equations, however, only for hybrid AC/DC grids with point-to-point and radial multi-terminal HVDC systems . An implementation based on the Julia language (PowerModules [19]) is presented in [12], however it has no control implemented. A unified converter model is presented in [3] which solves OPF in a single frame of reference, however the model adds additional components to the system, and the resulting Y_{bus} matrix is variable and needs to be recalculated at each optimization iteration, which may have implications for the speed of the optimization.

In recent years, several relaxation techniques have also been presented in the literature for AC [20] [21] [22] [23] [24], as well as for the hybrid AC/DC OPF problem, aiming to reduce the complexity of the problem and potentially ensure global optimal solutions. Notably, for AC/DC systems, the quadratic convex, second order cone and semidefinite relaxations of [25], [9], [10] and [1] can be mentioned. The relaxations, however, will not provide exact solutions. Deep neural networks have also been proposed recently for the OPF problem in AC grids [26] [27], however, to the best of our knowledge, no solution is yet available for hybrid AC/DC systems, and the results are not exact, leading to some optimality gap.

A. Motivations and main differences with the existing works

As can be seen above, existing tools often rely on approximations or simplifications, or sequential solutions of AC and DC equations, or need extensive libraries for modelling different components. Universal models can potentially solve many of these issues, however to the best of our knowledge, those reported in the literature either lack provisions of voltage and power control, or are limited to specific network topologies (e.g., point-to-point or radial MTDC), or are complex and therefore could have lower performance . Therefore, the motivation of this work is to addresses the limitations identified in the previous works by introducing a novel efficient universal model called Simple AC/DC bRAnch model (*SADRA*), for effective and simple modelling of AC/DC systems. Building on our previous work [3], *SADRA* offers several advantages compared with the rest of the literature as detailed below:

- It offers a unified approach for modelling diverse AC, DC and AC/DC elements including VSC and VSC interfaced elements (including point-to-point and multi-terminal HVDC), AC and DC lines, phase-shifter Transformers (PST), Controlled Tap-changing Transformers (CTT), and in general hybrid AC/DC systems, in a simple model; and therefore:
- It eliminates the need to develop separate models;
- It directly links AC and DC grids and therefore sequential solutions of AC and DC equations are NOT needed;
- It leverages conventional AC equations for modeling;
- It enables inclusion of voltage and power control into the optimization problem;
- It is flexible, scalable and robust and can be solved using different solvers;
- Compared to [3], it is simpler, more compact and significantly more efficient.

Moreover, since *SADRA* is based on conventional AC OPF formulation, any convexification or approximation applied to AC systems can be extended to the *SADRA* approach as well.

B. Main Contributions

The key contributions of this paper can be summarized as below:

- *Generalized Electrical Model for Hybrid AC/DC Grids:* We have shown that using the new universal model of *SADRA*, a generalized electrical model for hybrid AC/DC grids can be obtained. The new converter model embedded in *SADRA* enables simple representation of a variety of VSC-based components in the system. Using this new model, we allow *everything* to be *modelled in AC*. We have then shown how a variety of AC, DC and AC/DC components can be modelled using this general framework.
- *Compactness and Efficiency of the Proposed Model:* One important distinction with other universal models is the simplicity of *SADRA*, and that it does not need additional impedances, nor does it lead to branch admittance matrices which are different from the standard branch model of MATPOWER. This leads to an efficient implementation, with speeds of more than 6 times faster compared to the existing literature, as shown later in the results section.
- *Incorporating Control Actions in the Same Universal Model:* modelling of control actions is another important aspect that we have demonstrated how can be done using *SADRA*. We have shown how the variables in *SADRA* can be used to implement different control actions on voltages and powers in a generic component, such as a VSC, PST or CTT. Due to its compact and simple structure, *SADRA* is able to implement these control actions efficiently, leading to improved performance compared to the existing literature with more than 30% speed increase.
- *Circuit modification, as a simpler alternative to mathematical relaxation:* using *SADRA*, we essentially "relax" the DC voltages to have a dummy phase angle or in other words, we relax them into phasors, similar to AC

voltages. This will in fact relax the entire DC grid into an AC one and thereafter everything is modelled and sorted uniformly. However, while this is ultimately equivalent to mathematical relaxation, it is done without any need for direct mathematical modification, in contrast to existing methods such as [9]. We have also shown how *SADRA* prevents the flow of reactive power into the relaxed DC grid.

- *Software/model design:* We have developed a simple and easy to use and understand model within the AIMMS optimization environment, providing a user-friendly and comprehensive tool for modeling hybrid AC/DC systems. We also have illustrated its application in several case studies to validate is functionality and demonstrate its speed and robustness. The model, which is made open-source [28], is supported by a step-by-step tutorial available in [29]. This design enhances accessibility and practical application.

The rest of the paper is organized as follows. Fist, *SADRA* model is presented and explained. Modelling of AC and DC components using *SADRA* is explained next, where we can see how it can be used to model different elements of a hybrid AC/DC power system. Then OPF formulation using *SADRA* is presented. VSC control modes are reviewed next, and finally simulation results for two very large power systems are presented and discussed.

II. *SADRA* Model

SADRA is an evolved version of the conventional AC branch model [30], whereby by adding a simple *dummy generator* g_{dc} at the *from* bus, modelling of hybrid AC/DC grids is made possible. It can also be regarded as an evolved, more efficient and more compact solution based on our previous work, FUBM [3], which in turn is an evolution of the VSC model of [31]. Fig. 1 shows the traditional VSC model (Fig1-(a)), the AC branch model (e.g. used in MATPOWER) (Fig1-(b)) and *SADRA* (Fig1-(c)). It can be seen that compared to the AC branch model, only a dummy generator is added to the *from* bus. In contrast with the traditional VSC models, both AC and DC grids are physically connected when modelled using *SADRA*, and therefore only AC OPF equations are used, with the addition of two constraints per VSC to keep the DC grid *DC* (i.e. with no reactive power flow), and to model the VSC losses, as will be explained in Section II-C.

While we will see the operation and details of *SADRA* in the subsection II-A in greater detail, it should be noted that M_c in Fig. 1(a) is equal to τ in Fig. 1(c). Also N is a complex number whose magnitude is

$$|N| = \tau = M_c \tag{1}$$

Compared to FUBM, *SADRA* offers several advantages. Notably, its simpler and more compact structure results in significantly faster computation times, as demonstrated in subsequent results. Unlike FUBM, which incorporates variable resistors and reactors, complicating the Y_{br} matrices, SADRA avoids these complexities.

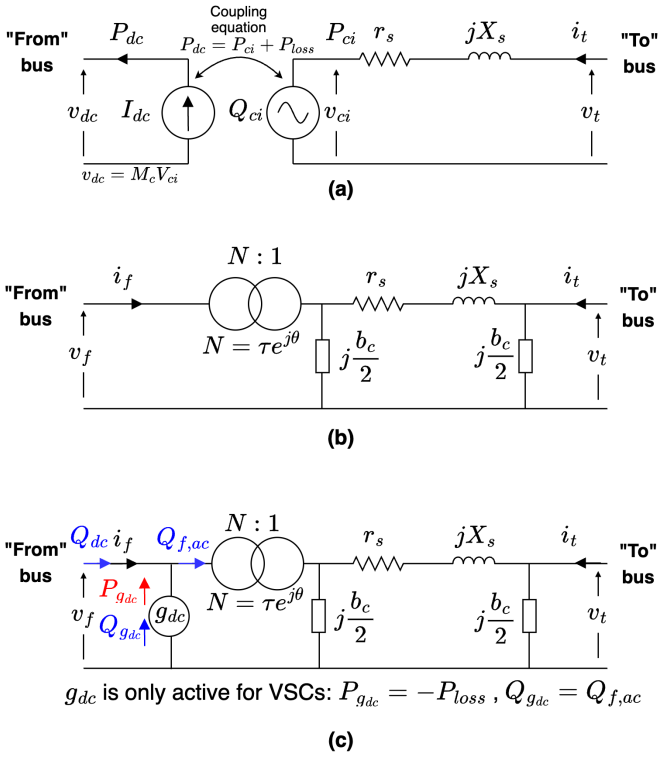

Fig. 1. a) traditional VSC model, b) MATPOWER branch model, c) proposed branch model (*SADRA*).

A. The model and its operation

As stated above, *SADRA* uses the AC branch model of MATPOWER and by a simple minimalistic modification of using a dummy generator enables modelling of VSCs and a range of other components, as well as possibility of modelling both AC and DC grids.

Similar to the AC branch model of MATPOWER, depending on what component is modelled, parts of the branch model of *SADRA* will be enabled or disabled as required.

B. Modelling AC and DC components

Fig. 2 shows how different DC, AC, or AC/DC components can be modelled. Modelling DC lines is simply done using only r_s, which represents the DC resistance of the DC line, as shown in Fig. 2-(a).

An AC π branch can be modelled using r_s, x_s and b_c (Fig. 2-(b)). Note that this is why both $jb_c/2$ shunt element of the conventional AC branch model of MATPOWER are kept in *SADRA* as well.

If only the dummy generator g_{dc} is disabled, *SADRA* becomes equivalent to the conventional AC model as shown in Fig. 2-(c). This again shows that *SADRA* can be used in a similar way to model any AC element. For example, a transformer can be modelled using a combination of r_s, x_s and the ideal transformer T with the complex tap ratio N (Fig.2-(d)).

Note that since N is a complex number, the model is capable of modelling tap-changing transformers as well as PSTs. Fig. 2-(e) and 2-(f) show a PST and a CTT, respectively.

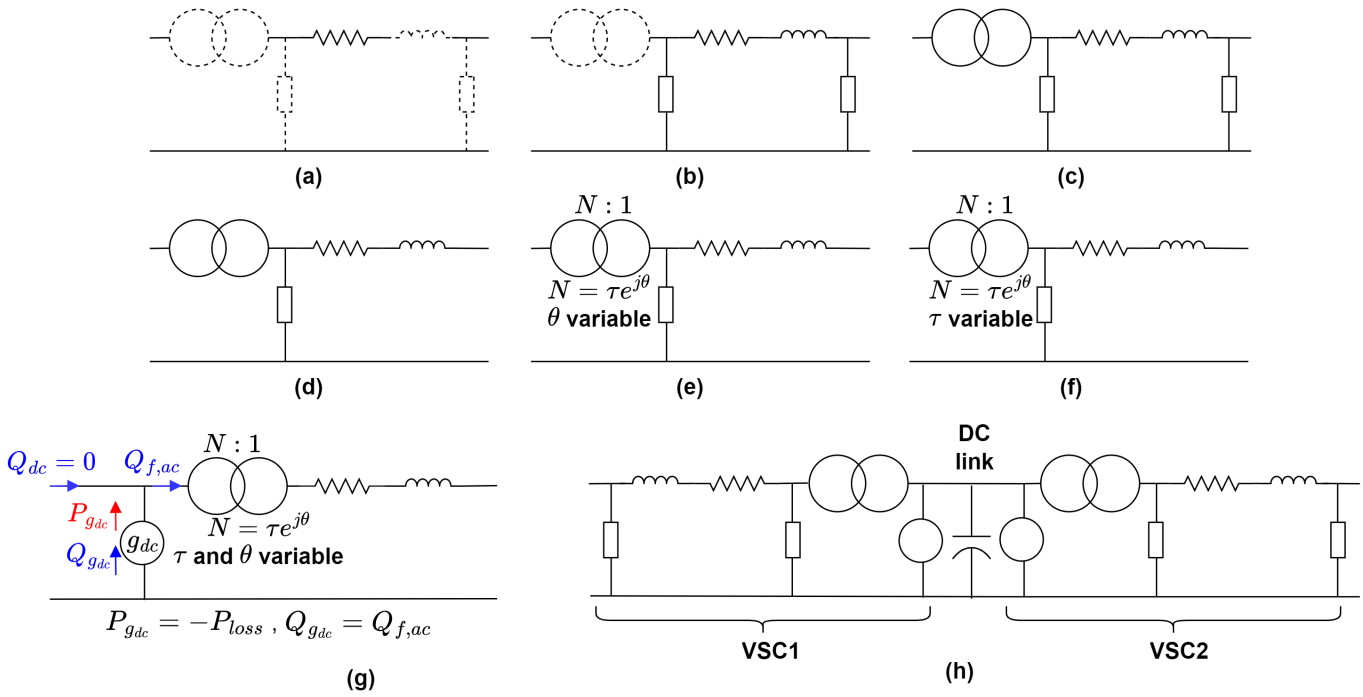

Fig. 2. *SADRA* models examples: a) dc line, b) ac line (*pi*) model, c) Matpower branch model, d) transformer model, e) PST, f) CTT, g) VSC, h) back-to-back VSC (e.g. UPFC).

$$N = \tau e^{j\theta} \tag{2}$$

R4: Note that (point 2)

As we will see later in the results section, not only *SADRA* is capable of modelling PSTs and tap changers, but it can also be used to model them as controlled elements in the optimization problem. For example, for modelling controllable PSTs, the phase shift θ will be considered as an optimization variable for the OPF problem, while the magnitude τ will be kept constant. In contrast, For CTTs, there won't be a phase shift ($\theta = 0$), while the magnitude τ will be taken as an optimization variable. That is why on the figures for CTT and PST, τ and θ are highlighted as *"variable"*.

C. Modeling VSCs and VSC-based components

The VSC (Fig. 2-(g)) can be modelled using the AC voltage generated at the VSC terminals as a result of its PWM control, by using the complex tap of the transformer where τ and θ model the amplitude modulation index and the phase shift action of the PWM, respectively [3]. There are two other important aspect in modelling the VSCs: modelling their power loss, and the link between AC and DC sides. In *SADRA*, we have a physical connection between the AC and DC sides, and the dummy generator guarantees that there will be no reactive power flow at the DC side and therefore the DC side remains truly DC. This is shown in Fig.2-(g) and can be also seen from equation (3) which is implemented as a constraint in the formulation:

$$Q_{g_{dc}} = Q_{f,ac} \longleftrightarrow Q_{dc} = 0 \tag{3}$$

The dummy generator also models the power loss of the converter. In this paper, we have used a quadratic loss equation as per IEC 62751-2 standard, as shown below, but as can be seen, modifying the model to incorporate any other loss model is easily possible:

$$P_{g_{dc}} = -\gamma|i_t|^2 - \beta|i_t| - \alpha \tag{4}$$

where γ, β, α are the loss coefficients of the converter.

It can be seen from Fig. 2(g) that using *SADRA*, we are essentially modelling everything in AC and therefore DC voltages (and currents) will also have a *"phase angle"*. This can be shown in relation to Fig. 1 using the equation below:

$$v_f = v_{dc}\angle\theta_{dc} \tag{5}$$

where θ_{dc} is the phase angle given to the DC side voltages (and currents) to convert - or relax- them into phasors.

This is in fact equivalent to relaxing the DC voltages to have *"phase angles"*. It is, however, different from the mathematical relaxation of [9], as here we have essentially relaxed the entirety of the *DC grid* into an AC one and are modelling and solving everything in AC, without direct mathematical modifications to the way the system is modelled or manipulating mathematical equations. Also it should be noted that convex relaxation of the model is not in the scope of this paper, and the resulting optimization problem remains non-convex. Overall, as a result of the above relaxation of DC voltages and currents, *SADRA* is applicable not only in point-to-point and radial MTDC, bus also in meshed grids as well.

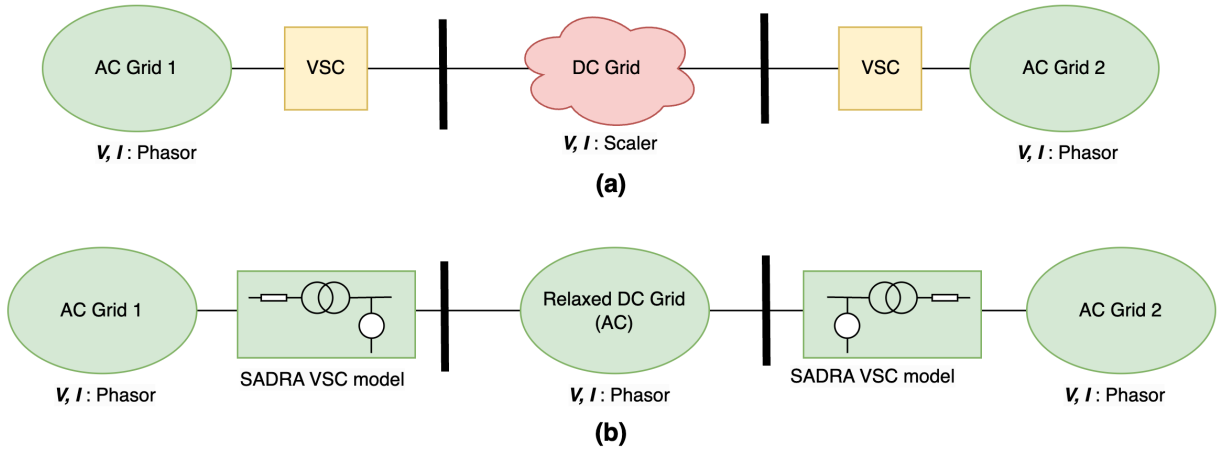

Fig. 3. a) An example AC/DC system (VSC-HVDC link), b) its modelling using *SADRA*. Green background means conventional AC equations apply.

The concept of DC *"phase angle"* and its effect is further explained below in Section II-D.

Finally, Fig.2-(h) shows an example of how more complex components such as those with back to back VSCs (for example a Unified Power Flow Controller - UPFC) can be implemented using *SADRA*. In this case, the two VSCs are each modelled using the VSC model of Fig.2-(g), with a DC link between them. Again, using *SADRA*, everything will be solved in AC.

D. Modelling hybrid AC/DC system using SADRA

Fig. 3 shows an example of how a hybrid AC/DC system, such as a point-to-point VSC-HVDC transmission link, can be modelled using *SADRA*. As mentioned above, the entire hybrid AC/DC grid is modelled and solved using AC equations. The DC voltages are relaxed to have a *phase angle*, which makes them similar to AC voltage phasors instead of scalars. This is in fact what allows the system modelled by *SADRA* to model the whole hybrid grid in AC. Note that this phase angle is the same for the whole relaxed DC grid. If multiple DC grids exist in the system, each one will have its own DC voltage phase angle. These phase angles are an artefact of relaxing the DC grid to become an AC one, and can be simply ignored when dealing with the results. Moreover, since DC grids do not have any reactances, no reactive power flows in them as all voltages and currents in a DC network have the same phase angle. Fig. 4 shows two generic connected DC buses, and the phasor diagram of their voltages and the current flowing between them. Since all the phasors have the same phase angle, therefore there won't be a reactive power flowing between them:

$$Q_{12} = |V_{12}||I_{12}|sin\theta_{12} = 0 \tag{6}$$

The dummy generators of the VSCs guarantee that there will not be any reactive power flowing into the DC grids, as there cannot be any in the DC grids, and hence they remain truly DC. Overall, it can be seen that using SADRA, there won't be any need to make a distinction between AC and DC grids, resulting in a unified model.

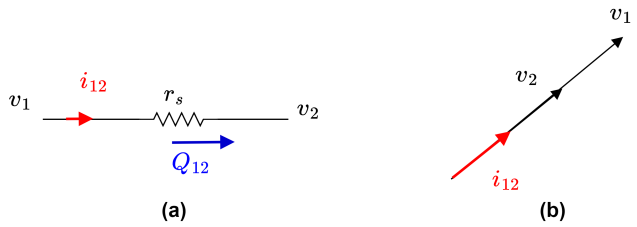

Fig. 4. a) two generic nodes in a relaxed dc grid b) phasor diagram of the voltages and current of (a).

E. Mathematical modelling of the hybrid AC/DC system

In this section, the modelling of the hybrid AC/DC system is presented. First, following MATPOWER's convention [30], the power balance equations for the hybrid AC/DC grid are presented. The 2×2 branch admittance matrix Y_{br} for *SADRA* (Fig.1-(c)) is exactly the same as that of MATPOWER (Fig. 1-(b)) and can be calculated using:

$$\begin{bmatrix} i_f \\ i_t \end{bmatrix} = Y_{br} \begin{bmatrix} v_f \\ v_t \end{bmatrix} = \begin{bmatrix} y_{ff} & y_{ft} \\ y_{tf} & y_{tt} \end{bmatrix} \begin{bmatrix} v_f \\ v_t \end{bmatrix} \tag{7}$$

$$Y_{br} = \begin{bmatrix} (y_s + \frac{jb_c}{2})\frac{1}{\tau^2} & -\frac{y_s}{\tau e^{-j\theta}} \\ -\frac{y_s}{\tau e^{j\theta}} & y_s + \frac{jb_c}{2} \end{bmatrix} \tag{8}$$

This already shows that while *SADRA* enables the modeling of AC/DC hybrid systems and a range of components includ-

ing VSCs, it has minimal additional complexity compared to the existing AC models.

For a network with n_b buses and n_l branches, the power injections can be calculated in matrix form as shown below. The four elements of the Y_{br} matrix for branch i are labelled as below and the corresponding elements of Y^i_{br} are used to form the four $n_l \times 1$ vectors Y_{ff},Y_{ft},Y_{tf} and Y_{ff}.

$$Y^i_{br} = \begin{bmatrix} y^i_{ff} & y^i_{ft} \\ y^i_{tf} & y^i_{tt} \end{bmatrix} \tag{9}$$

The sparse branch connection matrices C_f and C_t are then defined with sizes of $n_l \times n_b$ where their elements take the value *1* when the branch element of *from* or *to* side connects with the corresponding bus. All other elements of C_f and C_t are *zero* [30]. The *to* and *from* complex powers then can be written as

$$S_f = [C_f V] Y^*_f V^* \tag{10}$$

$$S_t = [C_t V] Y^*_t V^* \tag{11}$$

where

$$Y_f = [Y_{ff}] C_f + [Y_{ft}] C_t \tag{12}$$

$$Y_t = [Y_{tf}]\, C_f + [Y_{tt}]\, C_t \tag{13}$$

These equations now describe the whole AC/DC grid and can be used in the OPF, which is detailed in the Section III. Before reviewing the OPF formulations, however, we will first examine different control types for VSCs in hybrid networks in the next subsection, as this is necessary to be able to model control actions using *SADRA*.

F. VSC control modes

In this section, the various control modes for VSCs are outlined, and their mathematical integration into the *SADRA* framework is demonstrated. Generally, depending on the control needs of hybrid AC/DC power systems, the VSCs of the power system can be configured to manage voltages, or active and reactive powers, or a combination of those.

VSCs in general have three different control types, as can be seen in Table I [3], [32].

TABLE I
VSC CONTROL TYPES

VSC Control Type	Constraint 1	Constraint 2
I	θ	v_{ac}
	P_f	Q_{ac} or v_{ac}
II	v_{dc}	Q_{ac} or v_{ac}
III	v_{dc} droop	Q_{ac} or v_{ac}

For each control type, two constraints can be associated. These constraints are shown in Table I. For example, control type III represents droop controlled VSCs, where there is a constraint on the droop controlled voltage according to the defined P-V droop curves for the converters, as well as another constraint for controlling the AC side voltages or reactive powers. Control type II is for converters that directly apply a control over the DC link voltage, and maintain this voltage at a reference. Those converters can still control one more quantity at the AC side, which again can be the reactive power or the AC side voltage. It is also possible for example to control both active and reactive powers at the AC side of a VSC of type I.

It should be evident that a specific set of rules must be adhered to during the implementation of MTDC grids or HVDC-Links to prevent operational issues. For example, since VSCs of type II directly control the DC link voltage, there cannot be more than one converter of this type in each DC grid [3] [32], otherwise they could compete for controlling the DC bus voltage at different values. For the same reason, if there is a VSC type II present in a DC grid, the rest of the converters must be of type I. It is however possible to have multiple droop controlled converters (type III) in a single DC grid, as well as any number of type I converters. Nevertheless, since type I converters do not exert any control over the DC link voltage, they cannot be the only type present in a DC network, and it is essential to incorporate at least one VSC type II or type III for voltage regulation.

Now that the modelling of the hybrid grid and the VSC control modes are explained, the modelling of OPF is detailed in the following section (Section III) . We will also see how the different VSC control types can be considered in the optimization modelling at the end of that Section.

III. OPF FORMULATION USING *SADRA*

The OPF formulations using *SADRA* for hybrid AC/DC systems is presented in this section. This formulation also includes the optional power and voltage controls discussed earlier.

The goal in an OPF is normally to minimize the total generation cost $f(x)$:

$$f(x) = \sum_{i=1}^{n_g} f_i(P_{g,i}) \tag{14}$$

where f_i functions are polynomial (usually quadratic) cost functions of individual generators i, n_g is the number of generators and $P_{g,i}$ is the cost of generation associated with generator i. Note that dummy generators associated with VSC buses have zero cost associated to them, however their active and reactive powers are part of the optimization variables, similar to other generators.

The definition of the required sets and indices used in the formulation are shown in Table III below.

The OPF can be expressed as follows, and the different variables are explained in the text that follows. Note that this is a complete but compact representation of the OPF problem in accordance with the formulation presented in [3].

A. Conventional AC OPF Equations

$$min \quad f(x) \tag{15}$$

$s.t.$

$$S^i(x) + S^i_d - S^i_g = 0 \quad \forall i \in \mathcal{I} \tag{16}$$

TABLE II
DEFINITION OF SETS

Set Elements	*Set Symbol*
Buses	$\mathcal{I}$
Branches	$\mathcal{L}$
PSTs	$\mathcal{I}_{pst}$
CTTs	$\mathcal{I}_{ctt}$
VSCs	$\mathcal{I}_{vsc}$
VSCs type I	$\mathcal{I}_{vsc\#I} \subset \mathcal{I}_{vsc}$
VSCs type II	$\mathcal{I}_{vsc\#II} \subset \mathcal{I}_{vsc}$
VSCs type III	$\mathcal{I}_{vsc\#III} \subset \mathcal{I}_{vsc}$

This equality constraint shows the classical active and reactive power balance equations for all buses where S^is are complex powers of each bus i and are elements of the $S_{bus}(x) = [V]I^*_{bus} = [V]Y^*_{bus}V^*$.

$$|S_f(x)^i| \leq S^i_l \quad \forall i \in \mathcal{L} \tag{17}$$

$$|S_t(x)^i| \leq S^i_l \quad \forall i \in \mathcal{L} \tag{18}$$

Eqs. (17) and (18) show the branch thermal limits and apply to all branches.

We also need eq. (19) to define a reference phase angle for the slack bus of the system:

$$\theta_s = 0 \quad \text{(for the slack bus } s\text{)} \tag{19}$$

B. SADRA Generator Equations

SADRA adds the Eqs. (20) and (21) to the traditional AC OPF model. Eq. (20) is how *SADRA* guarantees that no reactive power flows through the DC grids and is applied to all VSC buses. This guarantees that the *"relaxed"* DC grid indeed remains DC, even after being physically connected to the rest of the AC grid.

$$Q^i_{dc}(x) = 0 \quad \forall i \in \mathcal{I}_{vsc} \tag{20}$$

Eq. (21) is used to take VSC losses into account. As discussed before, we have used quadratic converter loss model [3] [33] as shown in that equation.

$$P^k_{g_{dc}} = -\gamma^k |i^k_t|^2 - \beta^k |i_t|^k - \alpha^k \quad \forall k \in \mathcal{I}_{vsc} \tag{21}$$

C. SADRA Optional Control Equations

To include optional control into the model, optional equations (22)-(24) can be activated when there are voltage or power controls in the system.

Eq. (22) is the optional constraint for active power control for PSTs and VSCs, where $P_{f,set}$ shows the required active power value for the controlled PST and VSCs.

$$P^i_f(x) = P^i_{f,set} \quad \forall i \in \mathcal{I}_{vsc} \text{ or } \mathcal{I}_{pst} \ , \ i \notin \mathcal{I}_{vscIII} \tag{22}$$

Similar to the above, Eq. (23) shows the reactive power control for CTTs or AC sides of VSCs, where $Q_{t,set}$ is the vector of set or reference reactive power values for CTTs and VSCs.

$$Q^i_t(x) = Q^i_{t,set} \quad \forall i \in \mathcal{I}_{vsc} \text{ or } \mathcal{I}_{ctt} \tag{23}$$

Eq. (24) is applied to all VSCs that are droop controlled, where k_d shows the droop coefficient, and $P_{f,ref}$ and v_{ref} are the reference active power and voltages for the droop control for the considered VSC buses (of type III: droop controlled).

$$P^i_f(x) = P^i_{f,ref} - k^i_d(v^i_f - v^i_{ref}) \quad \forall i \in \mathcal{I}_{vscIII} \tag{24}$$

Therefore, it can be seen that all different VSC types can be modelled using these equations.

D. Vector Variables and Bounds

The vector of variables x is:

$$x = [P_g, \ Q_g, \ V_a, \ V_m, \ \theta, \ \tau]^T \tag{25}$$

And finally it should be noted that the variables may have upper and lower bounds (e.g. due to physical and operational requirements), which can be shown as below:

$$x_{min} \leq \ x \leq \ x_{max} \tag{26}$$

IV. CASE STUDY AND SIMULATIONS

While many of the comparable studies have studied relatively small systems up to 118 buses (e.g. [1] [17] [16] [18] [10]), in this study and in order to demonstrate both the performance and scalability of the *SADRA* model, we have considered two very large systems with up to 3120 buses. One of these systems is studied to show the performance of *SADRA*, while the other one is used to show how control actions can be implemented in *SADRA*. In the following, these systems, and their comparison against the literature are provided and the results discussed.

A. The extended 3120 bus AC/DC case representing the Polish system

The very large extended 3120 bus AC/DC case representing the Polish system with an interconnected 5 node MTDC grid is taken as the test case here. This system has 3120 AC and 5 DC buses, 3703 lines and 505 generators (of which 500 generators are from the system, and 5 are dummy generators used for modelling VSCs in *SADRA*). The data for AC and DC grids can be found at [34]. All simulations are solved in AIMMS, which is an optimization software that supports a wide range of mathematical optimization problems and provides access to multiple solvers such as IPOPT and CONOPT.

AIMMS is a powerful tool for optimization and its user friendly graphical interface makes it easy to use for implementation of optimization problems, with minimum coding required. A fully functional model of AC OPF and its explanation were previously published in AIMMS Academy website and is available for the interested readers in [29]. Moreover, the

AIMMS implementation of *SADRA* is also made open source and freely available at [28].

The tests were run on a MacBook Pro M2 3.2 GHz 2022, but as AIMMS only runs in a Windows environment, it was run using a Parallels ARM Virtual Machine with 6 GB of RAM on Windows 11. In order to have a fairer comparison, the Julia implementation of [12] and AIMMS implementation of [3] were also run on the same virtual machine.

The implementation of this system resulted in an optimization problem with 84027 constraints and 77087 variables. Table III shows the comparison of the results with those reported using PowerModelsACDC [12] and FUBM [3]. Two different solvers are tested for *SADRA* and for fairness for FUBM. For the PowerModelsACDC results, the results reflect on the total time from problem setup to obtaining the final solution, to have a fair comparison against the results of *SADRA* and FUBM. Note that [12] reported using Ipopt to solve the SOC model and Mosek for the SDP models. For completeness, we have included the results of both Ipopt, and competitive solver Gurobi for the relaxed models. It is worth to highlight that, in [12] Mosek was used for the SDP, and while it was shown that SDP formulation is generally tight, it was sensitive to numerical results, and for the large systems, including the 3120 bus system studied here, numerical issues were reported. Our tests also resulted in the same problem, and therefore the results of SDP with Mosek are not added in the results.

As it can be seen in Table III, *SADRA* reaches exactly the same values as reported in [12] and [3] for the NLP models. This both confirms the correctness of the developed and implemented models, as well as the accuracy of *SADRA*. *SADRA* required much fewer iterations compared to all studied models, except for the Gurobi QC model, which needed only two fewer iterations. Moreover, the results show that *SADRA* can be up to 6.28 times faster than FUBM when they are both run on the same machine. This can be attributed to the simpler structure of *SADRA* compared with FUBM, as discussed in Section II.

SADRA is only slightly slower than the results of NLP of [12], however, the results are comparable. It should be noted that [12] models are implemented in Julia programming language which is known for its speed, while *SADRA* is implemented in AIMMS which is a general-purpose optimization software, because of its ease of use and implementation. As expected, *SADRA* as well as the NLP formulation of [12], are both slower than the Quadratic Convex (QC) and Second order Cone (SOC) relaxed models than are solved using Gurobi. However it should be noted that *SADRA* (similar to the NLP formulation of PowerModelsACDC) gives exact results, while the above mentioned convex relaxations result in some inaccuracy (or "optimality gaps") in their final solutions. Overall, *SADRA* is shown to be faster in terms of number of iterations compared to all of these methods, and also faster in terms of time of solve compared with most of these methods, while giving exact solutions. Finally, it can be seen that *SADRA* performs well irrespective of the solver used, which shows its versatility.

B. Modified PEGASE system for evaluating the control actions

For evaluating the implementation of control actions, the modified PEGASE system of [3] is used and the results are compared. The original AC case contains 1354 buses, 260 generators and 1991 branches, from the Pan European Grid Advanced Simulation and State Estimation (PEGASE) project [35]. Figure 5 shows how the original system is modified to include two DC sub-grids: one HVDC link and one MTDC grid. Both DC grids operate at 345 kV nominal voltage.

There are overall 5 VSCs in this system, and their control types and constraints are shown in Table IV. It is worth highlighting that the second constraint of VSC 5 is left as a free variable to show that the control constraints are set individually and that the model is not restricted to them.

The results shown below confirm that this is the case for *SADRA* as well. Also, in the modified system of [3], two of the existing transformers were set as a PST and a CTT for controlling power and voltages respectively. All these controls are implemented in *SADRA* using the appropriate control constraints of (22)-(24).

The ensuing optimization problem which is again modelled in AIMMS and was run on the same machine, has 42738 constraints and 39255 variables. Detailed values of VSC voltages and powers are shown in Tables V and VI, and show that the control constraints of Table IV are successfully met. The control actions of the CTT and PST are also shown in the same table, and it can be verified that they are also successfully implemented. A check-mark is added in Tables V and VI against controlled voltages or powers to show that they are correctly controlled, in accordance with the control references of Table IV.

DC lines powers of the two DC networks of the studied case at the from sides are also provided in Table VII for completeness. These results overall prove once again that the *SADRA* model is implemented correctly.

Table VIII shows the comparison of solution and performance while using FUBM [3] and *SADRA*. It can be verified

TABLE III
COMPARISON OF AC/DC OPF RESULTS AGAINST THE LITERATURE

Model	NLP [12]	QC [12]		SOC [12]		FUBM [3]		*SADRA*	
Solver	IPOPT 3.14	IPOPT 3.14	Gurobi 11.0	IPOPT 3.14	Gurobi 11.0	CONOPT 4.1	IPOPT 3.11	CONOPT 4.1	IPOPT 3.11
Cost	2142635	2131071	2131071	21310962	2122752	2142635	2142635	2142635	2142635
Iterations	74	143	55	164	92	106	240	124	57
Time [s]	25.59	63.67	20.05	30.63	13.93	83.26	203.38	75.52	32.38

TABLE IV
CONTROL SETTINGS FOR VSC AND TRANSFORMERS [3]

Converter	Type	Constraint 1	Constraint 2
VSC1	I	Theta=0	$V_{ac} = 1.08$
VSC2	III	Droop controlled	$V_{ac} = 1.075$
VSC3	II	$V_{dc} = 1.01$	$V_{ac} = 1.06$
VSC4	I	$P_f = -500MW$	$V_{ac} = 1.07$
VSC5	I	$P_f = -450MW$	$V_{ac} = free$
Transformers	From	To	Constraint
PST	B7466	B3649	$P_f = -1.73$
CTT	B6153	B6807	$V_t = 1.1$

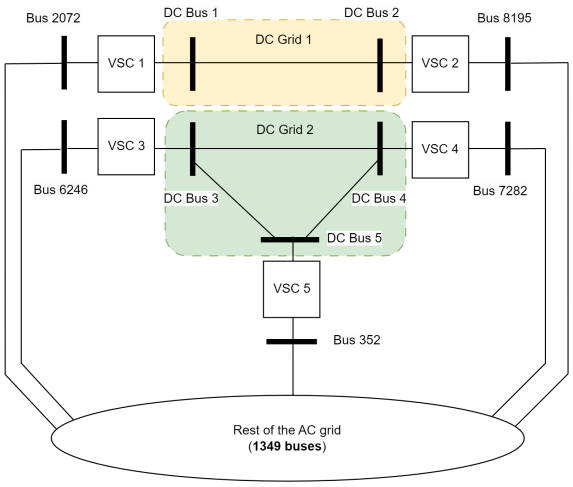

Fig. 5. Modified PEGASE system [3]. This system contains 1354 AC buses. The two DC subsystems and their connection to the rest of the AC system is shown here.

that *SADRA* has reached to the same exact solution, in fewer number of iterations and less time. IPOPT was chosen as the solver, as it faster compared with CONOPT, although the solutions were the same.

This proves *SADRA*'s performance in terms of implementing the controls, and shows that it can be used as a simple and easy to implement, yet powerful tool for modelling hybrid AC/DC systems.

C. Overall Comparison and future works

Table IX aims to summarize the quantitative results shown above, to provide an overall comparison of *SADRA* with comparable tools, namely with FUBM and PowerModelsACDC. As it could be seen from the results, PowerModels and *SADRA* provide up to an order of magnitude improvement in terms of speed over FUBM. PowerModelsACDC is slightly faster than *SADRA* for one of the modelling methods, and slower in two other models, when both are run on the same machine. It should nevertheless be mentioned that they are implemented using different software, with PowerModelsACDC implemented in Julia which is know for its speed [36], while *SADRA* is implemented in AIMMS which offers a user friendly interface for simple and easy implementation of optimization problems. Nevertheless, their speed is comparable. However, *SADRA*, like FUBM, provides a universal model which is able to model a variety of components, as well as control actions. As far as the author knows, this is not possible in PowerModelsACDC, or in fact in any other models.

Overall, this shows that *SADRA* is a powerful and useful tool for researchers and software developers working on the study of hybrid AC/DC systems.

Future works already being considered include convex relaxation of OPF modelled by *SADRA*, implementing and publishing *SADRA* as a PowerModels/PowerModelsACDC package for ease of access for researchers who use those software, and modelling failures in contingency situations for having a security constrained OPF.

V. CONCLUSION

This paper presented *SADRA*, a universal AC/DC branch model, and explored its use in OPF for hybrid AC/DC systems. *SADRA* is shown to be fast, versatile and easy to use. It allows modelling of a variety of AC and DC elements including AC and DC lines, phase-shifter transformers, controlled tap-changing transformers, VSCs and VSC interfaced elements (including point-to-point and multi terminal HVDC), and in general hybrid AC/DC systems, in a compact model, and directly links AC and DC grids where conventional AC equations can be used for modelling. Moreover, *SADRA* easily enables inclusion of voltage and power control capabilities to the optimization problem. Via simulations of OPF for large AC/DC power systems of up to 3120 buses using different solvers, its flexibility and scalability are demonstrated. *SADRA* is shown to be up to more than 6 times faster that the comparable universal model. It is also as fast as other methods in the literature while providing the important added capabilities of modelling control actions and a universal approach.

REFERENCES

[1] Mohamadreza Baradar, Mohammad Reza Hesamzadeh, and Mehrdad Ghandhari. Second-order cone programming for optimal power flow in vsc-type ac-dc grids. *IEEE Transactions on Power Systems*, 28:4282–4291, 2013.

[2] Yang Li, Yahui Li, Guoqing Li, Dongbo Zhao, and Chen Chen. Two-stage multi-objective opf for ac/dc grids with vsc-hvdc: Incorporating decisions analysis into optimization process. *Energy*, 147:286–296, 2018.

[3] Abraham Alvarez-Bustos, Behzad Kazemtabrizi, Mahmoud Shahbazi, and Enrique Acha-Daza. Universal branch model for the solution of optimal power flows in hybrid ac/dc grids. *International Journal of Electrical Power and Energy Systems*, 126:106543, 2021.

[4] Junyi Zhai, Xinliang Dai, Yuning Jiang, Ying Xue, Veit Hagenmeyer, Colin N. Jones, and Xiao Ping Zhang. Distributed optimal power flow for vsc-mtdc meshed ac/dc grids using aladin. *IEEE Transactions on Power Systems*, 37:4861–4873, 2022.

[5] Ali Raza, Ali Mustafa, Kumars Rouzbehi, Mohsin Jamil, Syed Omer Gilani, Ghulam Abbas, Umar Farooq, and Muhammad Naeem Shehzad. Optimal power flow and unified control strategy for multi-terminal HVDC systems. *IEEE Access*, 7:92642–92650, 2019.

[6] G. Buigues, V. Valverde, A. Etxegarai, P. Eguía, and E. Torres. Present and future multiterminal hvdc systems: Current status and forthcoming developments. *Renewable Energy and Power Quality Journal*, 1:83–88, 2017.

[7] Guadalupe Arcia-Garibaldi, Pedro Cruz-Romero, and Antonio Gómez-Expósito. Future power transmission: Visions, technologies and challenges, 2018.

TABLE V
COMPARISON OF OPTIMIZATION RESULTS: VSC AC AND DC VOLTAGES

	FUBM [3]				*SADRA*			
VSCs	$\|V_{dc}\|$	V_{dc} *"phase angle"*	$\|V_{ac}\|$	V_{ac} phase angle	$\|V_{dc}\|$	V_{dc} *"phase angle"*	$\|V_{ac}\|$	V_{ac} phase angle
VSC1	1.00002	-0.0517	1.08 ✓	-0.0505	1.00002	-0.0517	1.08 ✓	-0.0505
VSC2	1	-0.0517	1.075 ✓	-0.1098	1	-0.0517	1.075 ✓	-0.1098
VSC3	1.01 ✓	-0.38638	1.06 ✓	-0.2220	1.01 ✓	0.0750	1.06 ✓	-0.2220
VSC4	1.013389	-0.38638	1.07 ✓	-0.1244	1.013389	0.0750	1.07 ✓	-0.01244
VSC5	1.013224	-0.38638	1.023338	0.03394	1.013224	0.0750	1.023338	0.03394
Transformers								
PST	-	-	1.073	-0.3149	-	-	1.073	-0.3149
CTT	-	-	1.1 ✓	-0.02386600282	-	-	1.1 (at B6807) ✓	-0.0238

A ✓shows a control action from IV correctly implemented.

TABLE VI
COMPARISON OF OPTIMIZATION RESULTS: OPTIMIZATION VARIABLES AND POWERS

	FUBM [3]			*SADRA*			
VSCs	P_f	τ	θ	P_f	τ	θ	$P_{g_{dc}}(-=P_{loss})$
	[MW]	[MW]		[MW]			
VSC 1	-4.00007	0.931990	0 ✓	-4.00	0.93199	0 ✓	-0.016
VSC 2	3.99	0.92807	0.05690	3.99	0.92807	0.056907	-0.011
VSC 3	946.93	0.96948	-0.52297	946.93	0.96948	-0.52297	-0.848
VSC 4	-500 ✓	0.93316	-0.19630	-500 ✓	0.93316	-0.19630	-0.225
VSC 5	-450 ✓	0.97607	-0.2454988	-450 ✓	0.97607	-0.2454988	-0.199
Transformers							
PST	-1.73 ✓	1 ✓	0.00014797	-1.73 ✓	1 ✓	0.000147	0
CTT	0.0726	0.95569	0 ✓	0.0726	0.95569	0 ✓	0
CTT	Voltage at the terminal (B6807):	1.1 ✓		Voltage at the terminal (B6807):	1.1 ✓		

A ✓shows a control action from Table IV correctly implemented.

TABLE VII
DC LINES' POWER P_f

	Line	1-2	3-4	4-5	5-3
FUBM	P_f [MW]	4.0000848	-481.7577382	16.64963983	466.6477501
SADRA	P_f [MW]	4.0000848	-481.7577382	16.64963983	466.6477501

TABLE VIII
COMPARISON OF THE SOLUTION AND PERFORMANCE WHEN CONSIDERING VSC CONTROLS.

Model	FUBM [3]	*SADRA*
OPF Solver	IPOPT 3.11	IPOPT 3.11
Iterations	70	66
Time [s]	25.11	17.03
Total Cost [$]	74037.8782	74037.8782

[8] Ehab E. Elattar, Abdullah M. Shaheen, Abdallah M. Elsayed, and Ragab A. El-Sehiemy. Optimal power flow with emerged technologies of voltage source converter stations in meshed power systems. *IEEE Access*, 8:166963–166979, 2020.

[9] Matthias Hotz and Wolfgang Utschick. Hynet: An optimal power flow framework for hybrid ac/dc power systems. *IEEE Transactions on Power Systems*, 35:1036–1047, 2020.

[10] Shahab Bahrami, Student Member, Francis Therrien, and Vincent W S Wong. Semidefinite relaxation of optimal power flow for ac – dc grids. *IEEE Transactions on Power Systems*, 32:289–304, 2017.

[11] Nico Meyer-Huebner, Michael Suriyah, and Thomas Leibfried. Distributed optimal power flow in hybrid ac-dc grids. *IEEE Transactions on Power Systems*, 34:2937–2946, 7 2019.

[12] Hakan Ergun, Jaykumar Dave, Dirk Van Hertem, and Frederik Geth. Optimal power flow for ac-dc grids: Formulation, convex relaxation, linear approximation, and implementation. *IEEE Transactions on Power Systems*, 34:2980–2990, 2019.

[13] Roger Wiget and Goran Andersson. Optimal power flow for combined ac and multi-terminal hvdc grids based on vsc converters. *IEEE Power and Energy Society General Meeting*, pages 1–8, 2012.

[14] Wang Feng, Anh Le Tuan, Lina Bertling Tjernberg, Anders Mannikoff, and Anders Bergman. A new approach for benefit evaluation of multiterminal vsc-hvdc using a proposed mixed ac/dc optimal power flow. *IEEE Transactions on Power Delivery*, 29, 2014.

[15] Johan Rimez and Ronnie Belmans. A combined ac/dc optimal power

TABLE IX
A COMPARISON BETWEEN MODELS AND IMPLEMENTATIONS

	Speed	Iterations to Solve	Control Actions	Universality
FUBM (AIMMS) [3]	-	-	+	+
PowerModelACDC (Julia/JuMP) [12]	+	+	-	-
SADRA(AIMMS)	+	++	+	+

flow algorithm for meshed ac and dc networks linked by vsc converters. *International Transactions on Electrical Energy Systems*, 25, 2015.
[16] Deepak Pullaguram, Ramtin Madani, Tuncay Altun, and Ali Davoudi. Optimal power flow in ac/dc microgrids with enhanced interlinking converter modeling. *IEEE Journal of Emerging and Selected Topics in Industrial Electronics*, 3:527–537, 2022.
[17] Tuncay Altun, Student Member, Ramtin Madani, Ali Davoudi, and Senior Member. Topology-cognizant optimal power flow in. *IEEE Transactions on Power Systems*, 36:4588 – 4598, 2021.
[18] Zhifang Yang, Haiwang Zhong, Anjan Bose, Qing Xia, and Chongqing Kang. Optimal Power Flow in AC-DC Grids with Discrete Control Devices. *IEEE Transactions on Power Systems*, 33(2):1461–1472, mar 2018.
[19] Carleton Coffrin, Russell Bent, Kaarthik Sundar, Yeesian Ng, and Miles Lubin. Powermodels.j1: An open-source framework for exploring power flow formulations. 2018.
[20] Christian Bingane, Miguel F. Anjos, and Sebastien Le Digabel. Tight-and-cheap conic relaxation for the AC optimal power flow problem. *IEEE Transactions on Power Systems*, 33(6):7181–7188, nov 2018.
[21] Steven H. Low. Convex relaxation of optimal power flow - Part i: Formulations and equivalence. *IEEE Transactions on Control of Network Systems*, 1(1):15–27, mar 2014.
[22] Steven H. Low. Convex relaxation of optimal power flow-part II: Exactness. *IEEE Transactions on Control of Network Systems*, 1(2):177–189, jun 2014.
[23] Carleton Coffrin, Hassan L. Hijazi, and Pascal Van Hentenryck. The QC Relaxation: A Theoretical and Computational Study on Optimal Power Flow. *IEEE Transactions on Power Systems*, 31(4):3008–3018, jul 2016.
[24] Daniel K. Molzahn and Ian A. Hiskens. A Survey of Relaxations and Approximations of the Power Flow Equations. *Foundations and Trends® in Electric Energy Systems*, 4(1-2):1–221, 2019.
[25] Hakan Ergun, Jaykumar Dave, Dirk Van Hertem, and Frederik Geth. Optimal Power Flow for AC-DC Grids: Formulation, Convex Relaxation, Linear Approximation, and Implementation. *IEEE Transactions on Power Systems*, 34(4):2980–2990, jul 2019.
[26] Xiang Pan, Minghua Chen, Tianyu Zhao, and Steven H. Low. Deepopf: A feasibility-optimized deep neural network approach for ac optimal power flow problems. *IEEE Systems Journal*, 17(1):673–683, 2023.
[27] Wanjun Huang, Xiang Pan, Minghua Chen, and Steven H. Low. Deepopf-v: Solving ac-opf problems efficiently. *IEEE Transactions on Power Systems*, 37(1):800–803, 2022.
[28] Mahmoud Shahbazi. Sadra, a universal ac/dc branch model for optimal power flow studies, 2024. https://github.com/mahmoudshahbazi/SADRA [Accessed: (14/08/2024)].
[29] Mahmoud Shahbazi. Optimal power flow (opf) in aimms, 2023. https://how-to.aimms.com/Articles/510/opf.html [Accessed: (14/08/2024)].
[30] Ray D Zimmerman and Carlos E Murillo-s. Matpower manual version 7.1. page 248, 2020.
[31] Enrique Acha, Pedro Roncero-Sánchez, Antonio De La Villa Jaén, Luis M. Castro, and Behzad Kazemtabrizi. *VSC-FACTS-HVDC: Analysis, modelling and simulation in power*. 2019.
[32] Runze Chai, Baohui Zhang, Jingming Dou, Zhiguo Hao, and Tao Zheng. Unified power flow algorithm based on the nr method for hybrid ac/dc grids incorporating vscs. *IEEE Transactions on Power Systems*, 31(6):4310–4318, 2016.
[33] Zhicheng Li, Jinghan He, Yin Xu, and Xiaojun Wang. An optimal power flow algorithm for ac/dc hybrid power systems with vsc-based mtdc considering converter power losses and voltage-droop control strategy. *IEEJ Transactions on electrical and electronic engineering*, 13(12):1690–1698, 2018.
[34] Johan Rimez and Ronnie Belmans. A combined ac / dc optimal power fl ow algorithm for meshed ac and dc networks linked by vsc converters. pages 2024–2035, 2024.
[35] Stéphane Fliscounakis, Patrick Panciatici, Florin Capitanescu, and Louis Wehenkel. Contingency ranking with respect to overloads in very large power systems taking into account uncertainty, preventive, and corrective actions. *IEEE Transactions on Power Systems*, 28(4):4909–4917, 2013.
[36] Jeffrey M Perkel et al. Julia: come for the syntax, stay for the speed. *Nature*, 572(7767):141–142, 2019.

Mahmoud Shahbazi (SM'19) is an Associate Professor in Electrical Engineering at Durham University, Durham, UK (ranked 78 in QS World University Rankings 2024). His research interests include modern energy systems reliability and resilience, fault-tolerant control, renewable integration and power system modelling and optimization . He has published over 50 research papers and has been involved as PI or Co-I in several projects with a combined worth of more than £14M.